Supporting information for:

Multiscale Analysis for Field–Effect Penetration through Two-Dimensional Materials

Tian Tian,[†] Peter Rice,[‡,¶] Elton J. G. Santos,[*,‡,¶] and Chih-Jen Shih[*,†]

[†]Institute for Chemical and Bioengineering, ETH Zürich, Zürich 8093, Switzerland

[‡]School of Mathematics and Physics, Queen's University Belfast, United Kingdom

[¶]School of Chemistry and Chemical Engineering, Queen's University Belfast, United Kingdom

E-mail: e.santos@qub.ac.uk; chih-jen.shih@chem.ethz.ch

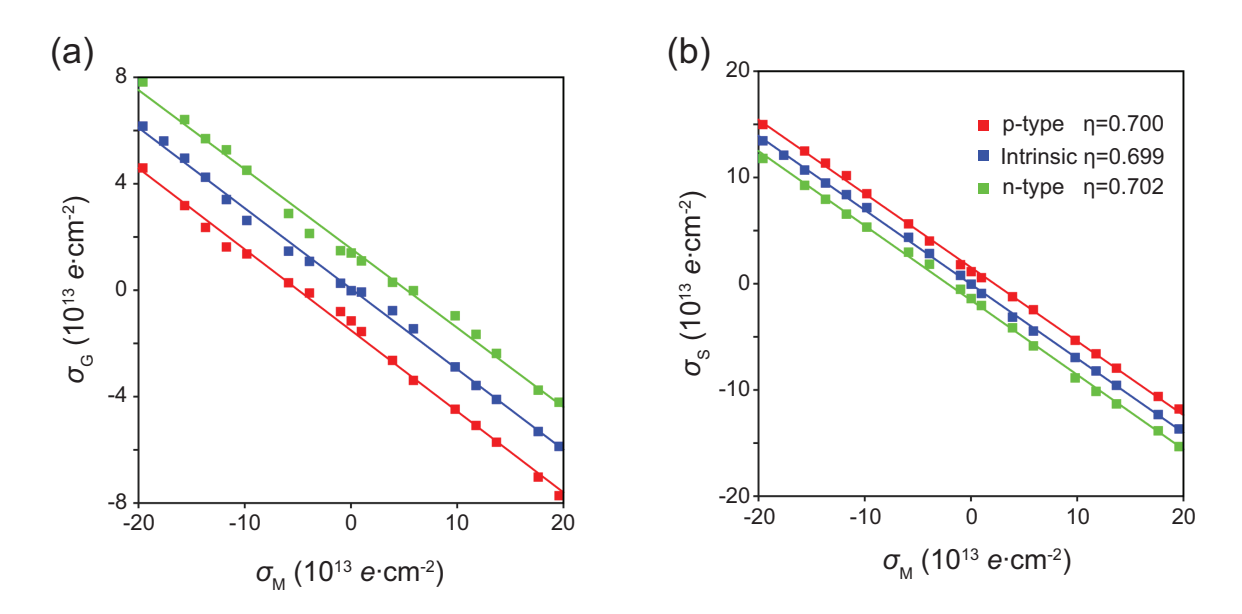# Additional Results from the First-Principles Calculations

Figure S1: Induced charge densities at (a) graphene, σ_{G}, and (b) Si(111), σ_{S}, as a function of σ_{M} in different systems: intrinsic (blue), p-type (green) and n-type (red) Si, respectively. The doping levels of Si are the same as in Figure 4 in the main body. σ_{M} ranges from -20×10^{13} $e{\cdot}\mathrm{cm}^{-2}$ to 20×10^{13} $e{\cdot}\mathrm{cm}^{-2}$. The η values are extracted by linear-fitting of the $\sigma_{\mathrm{S}} - \sigma_{\mathrm{M}}$ curves.
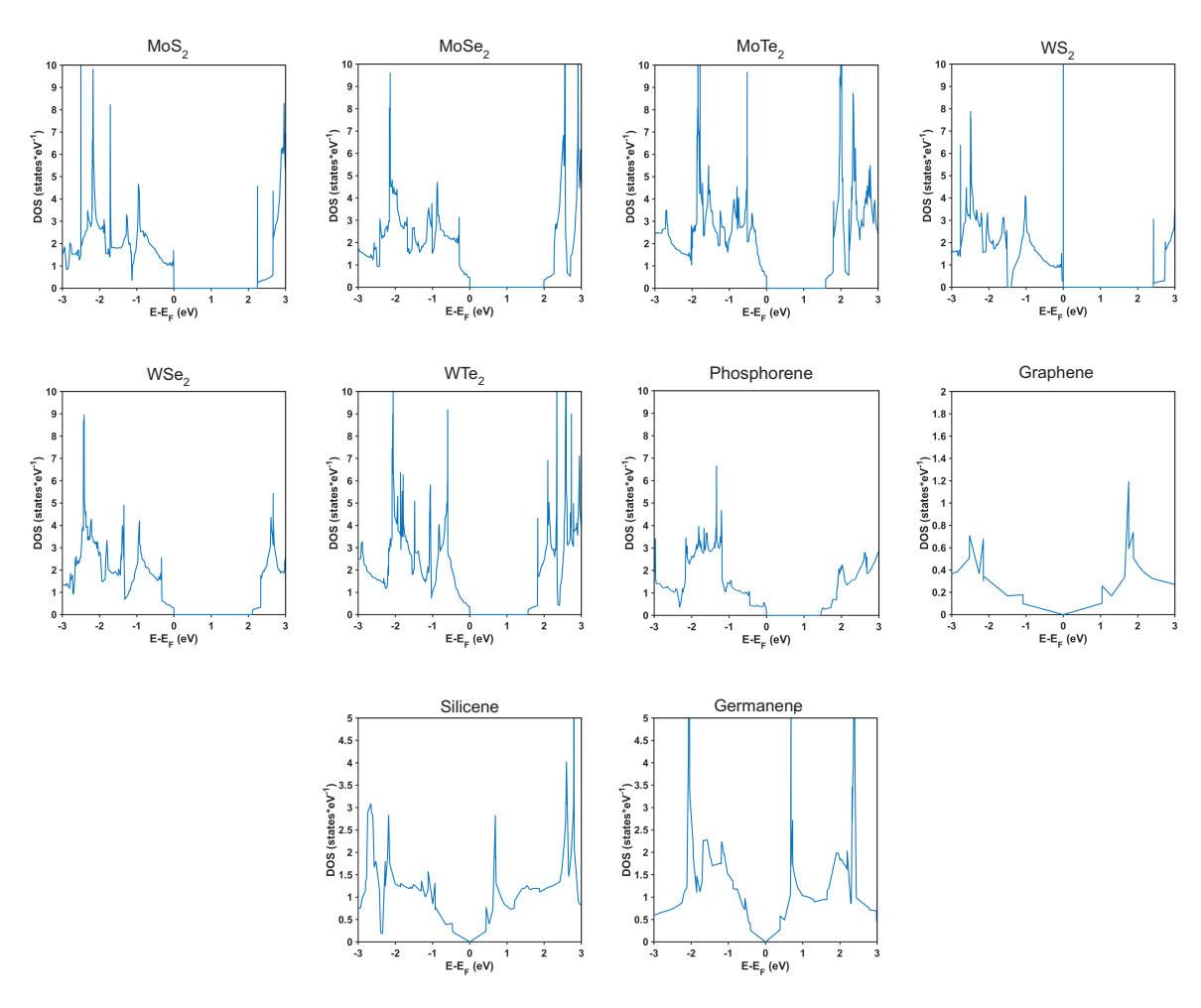
Figure S2: Density of states as a function of relative energy level of several selected 2D materials (MoS$_2$, MoSe$_2$, MoTe$_2$, WS$_2$, WSe$_2$, WTe$_2$, phosphorene, graphene, silicene and germanene) by HSE06 hybrid functional method.

Effect of interface States on the Transparency of Mono-layer 2D Materials

Here we model how the interface states at the 2D material-semiconductor interface influence the performance of a MOGS QC, including their effect on the transparency of monolayer 2D materials. We consider a classical model which assumes the interface states are atomically thin on the semiconductor surface and are completely ionized species.[S1–S3] The schematic illustration for the graphene-semiconductor interface considering the interface states can be found in Figure S3. The interface states possess a constant charge density of σ_{is}, which is
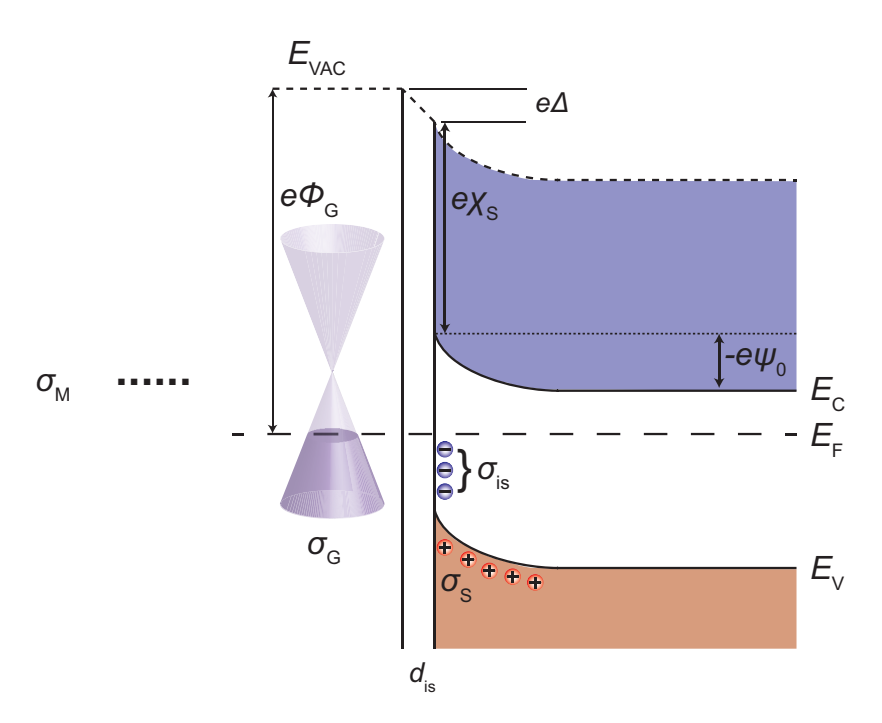

Figure S3: Scheme for the graphene-semiconductor interface with interface states.

a function of the interface density of states D_{is} and the neutral energy level of the interface states. The interface states create a potential drop Δ over the interface layer, which has a width of d_{is} and permittivity ϵ_{is}. According to Gauss's law, Δ is dependent on both σ_{is} and σ_S:

$$\Delta = d_{\mathrm{is}}\frac{\sigma_{\mathrm{S}} + \sigma_{\mathrm{is}}}{\epsilon_{\mathrm{is}}} \tag{1}$$

The potential drop results in a deviation from the Schottky-Mott rule, which is given by:

$$\Delta = \frac{E_{C,\infty} - E_{F,\infty}}{e} + \chi_S - \psi_0 - \phi_G \tag{2}$$

Combining eqs 1 and 2, it follows:

$$d_{is}\frac{\sigma_S + \sigma_{is}}{\epsilon_{is}} = \frac{E_{C,\infty} - E_{F,\infty}}{e} + \chi_S - \psi_0 - \phi_G \tag{3}$$

Following the same procedure of eq 10 in main text, the transparent index η is given by:

$$
\begin{aligned}
\eta &= -\frac{\partial \sigma_S}{\sigma_M} \\
&= -\frac{\partial \sigma_S}{\partial \psi_0}\frac{\partial \psi_0}{\partial \phi_G}\frac{\partial \phi_G}{\sigma_G}\frac{\partial \sigma_G}{\partial \sigma_M} \\
&= \frac{C_S}{C_G}\frac{\partial \psi_0}{\partial \phi_G}(\eta - 1) \\
&= \frac{1}{1 - \frac{C_G}{C_S}\frac{\partial \phi_G}{\partial \psi_0}} \\
&= \frac{1}{1 + k\frac{\partial \phi_G}{\partial \psi_0}}
\end{aligned}
\tag{4}
$$

Compared to eq 10 in main text, the factor $k = -\dfrac{\partial \phi_G}{\partial \psi_0}$ is given by eq 3:

$$
\begin{aligned}
k &= -\frac{d_{is}}{\epsilon_{is}}\left(\frac{\partial \sigma_{is}}{\partial \psi_0} + \frac{\partial \sigma_S}{\partial \psi_0}\right) + 1 \\
&= \frac{d_{is}}{\epsilon_{is}}C_S + 1
\end{aligned}
\tag{5}
$$

Finally we obtain the expression for the transparency through a monolayer graphene when the interface states are considered, as follows:

$$
\begin{aligned}
\eta &= \frac{1}{1 + k\dfrac{C_{\mathrm{G}}}{C_{\mathrm{S}}}} \\
&= \frac{1}{1 + \dfrac{d_{\mathrm{is}}}{\epsilon_{\mathrm{is}}}C_{\mathrm{G}} + \dfrac{C_{\mathrm{G}}}{C_{\mathrm{S}}}} \\
&= \frac{1}{1 + \dfrac{C_{\mathrm{G}}}{C_{\mathrm{is}}} + \dfrac{C_{\mathrm{G}}}{C_{\mathrm{S}}}}
\end{aligned}
\tag{6}
$$

Note that the final expression for η is independent of σ_{is}. Instead, the governing parameter is the geometric capacitance of the interface layer $C_{\mathrm{is}} = \dfrac{\epsilon_{\mathrm{is}}}{d_{\mathrm{is}}}$. Accordingly, the transparency when considering the interface layer is always lower than that in the ideal case (when $d_{\mathrm{is}} = 0$). On a clean semiconductor surface, d_{is} is as low as 0.4-0.5 nm. Since ϵ_{is} is larger than ϵ_0, we infer that C_{is} is comparable to C_{G}. On the other hand, when the interface layer is thicker (e.g. long-chain hydrocarbon adsorption), C_{is} is much lower than that on a clean semiconductor surface, thereby resulting in a lower transparency. The above analysis would also be valid for other 2D materials (by substituting C_{G} with the general term C_{Q}).

We would like to point out that the above model is derived under the assumption that σ_{is} is constant and independent of σ_{S} and σ_{G}, which might not be very realistic. More experimental results are required to gain better insights at the interface.

Modeling the Penetration through Multilayer Graphene in a MOGS QC

In this section we propose a simplified model for the penetration of an electric displacement field through multilayer graphene in a MOGS QC. The interfacial coupling is ignored and each layer possesses the same electronic property, as schematically illustrated in Figure S4.
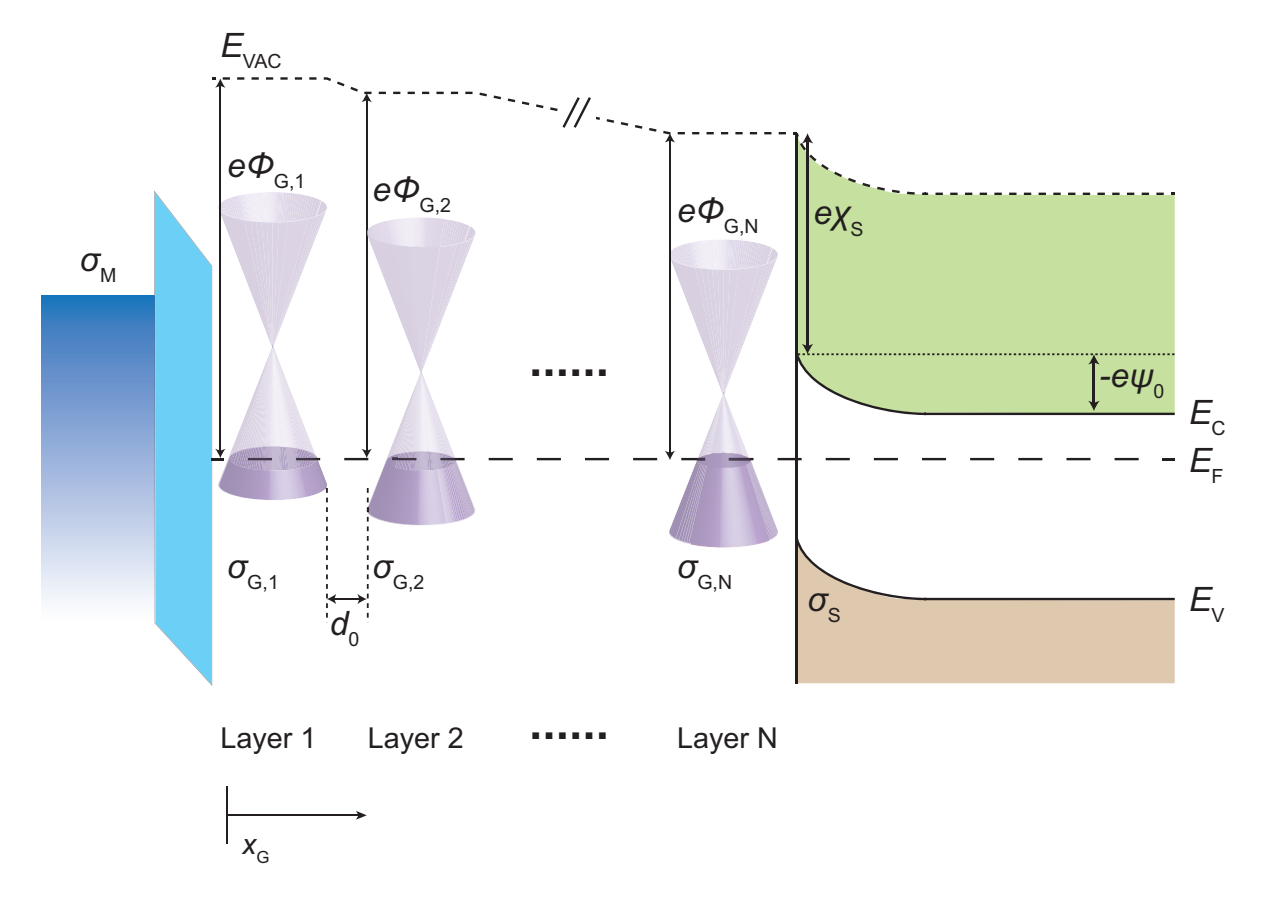

Figure S4: Schematic for the multilayer graphene MOGS QC system

We assume that each graphene layer is separated by a distance d_0 (ca. 0.33 nm) with permittivity of ϵ_G (taken the value of graphite,[S4,S5] $\epsilon_G \approx 2.4\epsilon_0$). We neglect the space between the first graphene layer and the oxide layer, as well as the interface states between the last graphene layer and the semiconductor layer. The electric fields in the oxide layer and the electric field at the semiconductor surface are $\mathscr{E}_{ox}$ and $\mathscr{E}_S$, respectively. The electric field between the i and $i+1$ graphene layer is expressed as $\mathscr{E}_{G,i}$. Consider a multilayer graphene

with layer number N, for the i-th graphene layer $\sigma_{G,i}$, Gauss's law suggests:

1. $i = 1$

$$\mathscr{E}_{ox}\epsilon_{ox} + \sigma_{G,1} - \mathscr{E}_{G,1}\epsilon_{G} = 0 \qquad (7)$$

2. $i = 2 \cdots N - 1$

$$\mathscr{E}_{G,i\text{-}1}\epsilon_{G} + \sigma_{G,i} - \mathscr{E}_{G,i+1}\epsilon_{G} = 0 \qquad (8)$$

3. $i = N$

$$\mathscr{E}_{G,N\text{-}1}\epsilon_{G} + \sigma_{G,N} - \mathscr{E}_{S}\epsilon_{S} = 0 \qquad (9)$$

Also note that the difference between the vacuum energy level E_{VAC} between i and $i+1$ graphene layers $(i = 1 \cdots N - 1)$ is identically the difference between the work function of the two layers:

$$\mathscr{E}_{G,i}d_0 = \phi_{G,i+1} - \phi_{G,i} \qquad (10)$$

The series of equations can therefore be solved numerically in a self-consistent approach by giving a initial value of $\mathscr{E}_{S}$.
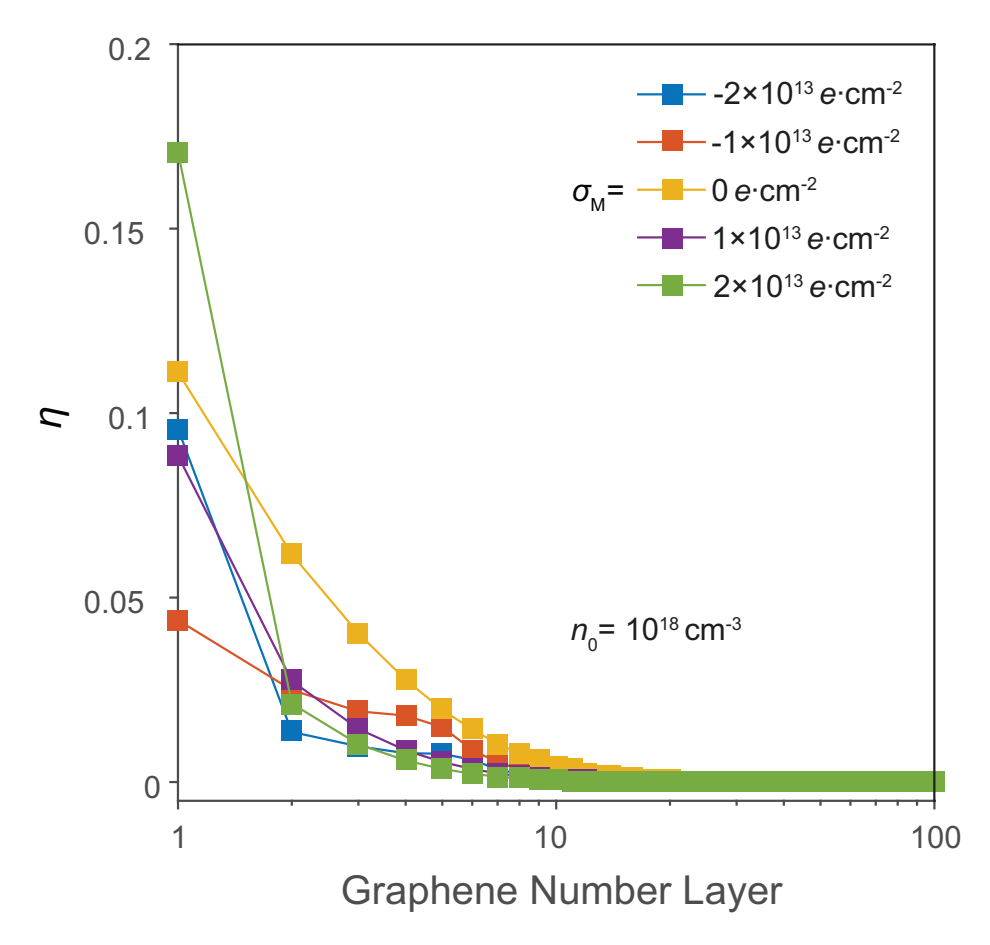
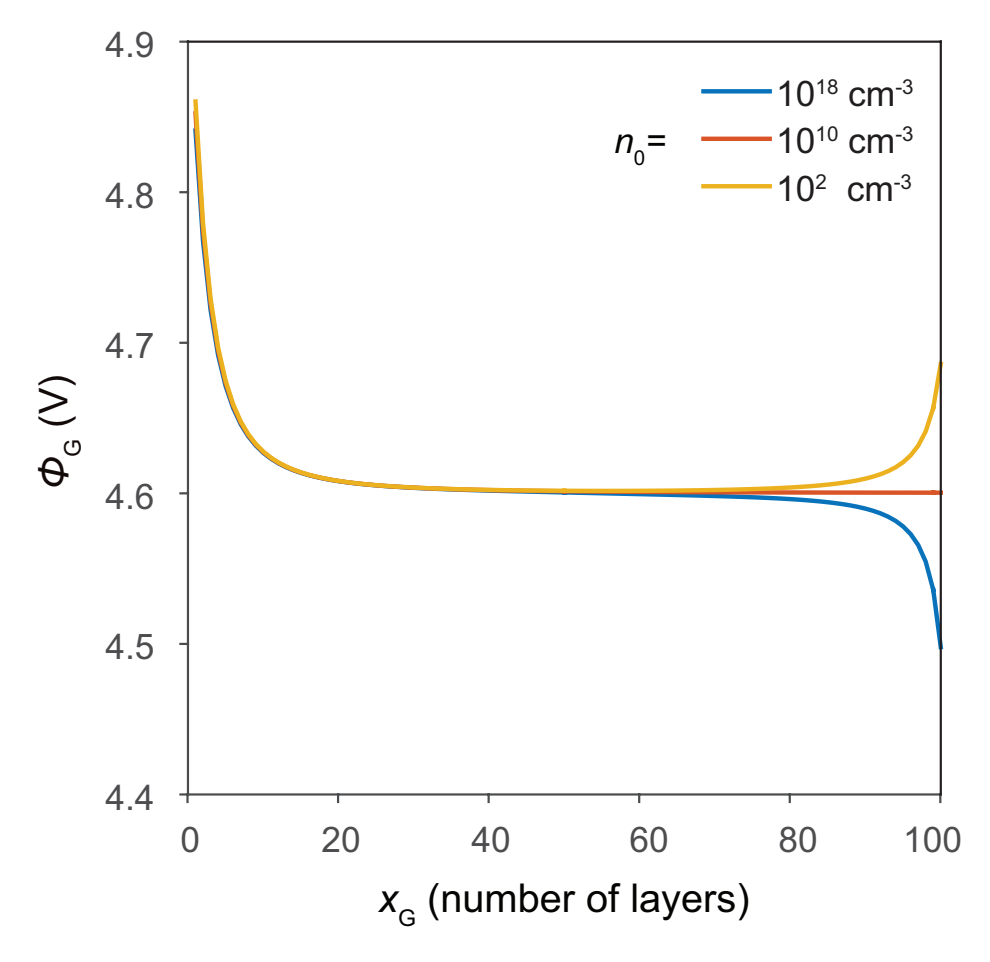Figure S5: Calculated transparency index η as a function of layer number N, corresponding to Figure 3b in main text.

Figure S6: The work function of 100-layer graphene as a function of distance from the oxide-graphene interface x_G (in number of layers), when $\sigma_M = -10^{13} \ e \cdot cm^{-2}$. Three cases are considered ($n_0 = 10^{18}$ cm^{-3}, $n_0 = 10^{10}$ cm^{-3} and $n_0 = 10^2$ cm^{-3}, respectively). The boundary layer of graphene with oxide remains indistinguishable while the boundary layer at the graphene-semiconductor interface is determined by the doping level of semiconductor. Away from the boundary layers, the graphene layers remains charge neutral ($\phi_G = 4.6 \ V$). These results indicate that the electric field can only penetrate into a limited length in multilayer graphene.

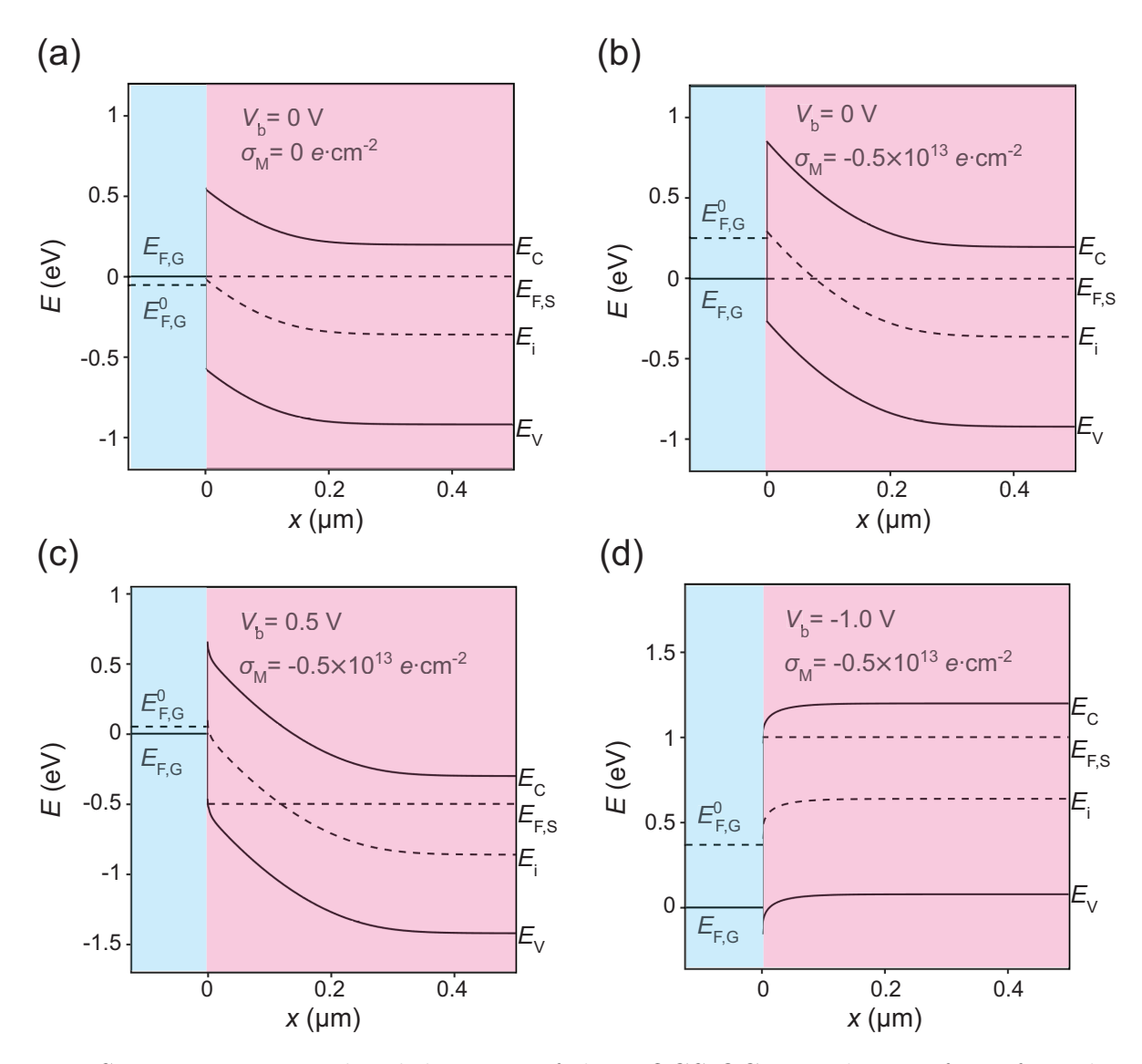# Band Diagrams of a MOGS QC under Different Conditions

Figure S7: Representative band diagrams of the MOGS QC near the interface of graphene (blue) and semiconductor (red), under various conditions: (a) $V_b = 0$ V, $\sigma_M = 0$ $e \cdot cm^{-2}$; (b) $V_b = 0$ V, $\sigma_M = -0.5 \times 10^{13}$ $e \cdot cm^{-2}$; (c) $V_b = 0.5$ V, $\sigma_M = -0.5 \times 10^{13}$ $e \cdot cm^{-2}$; (d) $V_b = -1.0$ V, $\sigma_M = -0.5 \times 10^{13}$ $e \cdot cm^{-2}$. The Si layer has a doping level of 10^{16} cm^{-3}. The $E_{F,G}$ is drawn in solid line and set to 0 eV, while the Fermi level at CNP, $E_{F,G}^0$ is demonstrated as dashed line. The Fermi level $E_{F,S}$, conduction band E_C, mid-gap E_i and valence band E_V energy levels of semiconductor are displayed, respectively.

To overview the macroscopic model, several representative band diagrams are drawn in

Figure S7 to explicate the influence of both gating and bias in a MOGS QC ($N_\mathrm{D} = 10^{16}$ cm^{-3} for the Si layer). The conduction band, valence band and mid-gap energy levels in semiconductor are described by (i) $E_\mathrm{C}(x) = E_{\mathrm{C},\infty} - e\psi(x)$, (ii) $E_\mathrm{V}(x) = E_{\mathrm{V},\infty} - e\psi(x)$ and (iii) $E_\mathrm{i}(x) = E_{\mathrm{i},\infty} - e\psi(x)$, respectively, where $\psi(x)$ is solved by applying boundary conditions $\psi(0) = \psi_0$ and $\psi(\infty) = 0$ for eq 3 in the main body. In the case of free contact (Figure S7a), the deviation between graphene's Fermi level $E_{\mathrm{F,G}}$ with the CNP Fermi level $E_{\mathrm{F,G}}^0$ indicates that a small degree of charge transfer readily takes place at the SG interface. When a negative σ_M of -0.5×10^{13} $e{\cdot}$cm^{-2} is applied (Figure S7b), the $E_{\mathrm{F,G}}$ significantly shifts due to the charge induction via the field effect. Note that the space charge at the SG interface is also tuned to weak inversion state from the depletion state at free contact, indicating the "penetration" of positive charge from the graphene 2DEG to the semiconductor layer. In Figure S7c, a reverse bias of 0.5 V is further applied in addition to Figure S7b. We observe that $E_{F,G}$ shifts back near the CNP of graphene, and a weak inversion layer at the SG interface is formed. This is a clear indication that bias can interfere with the gate control by σ_M. On the other hand, at the forward bias regime when a $V_\mathrm{b} = -1.0$ V is applied (Figure S7d), an accumulation layer is generated at the SG interface, and the $E_{F,G}$ is observed to move away from $E_{\mathrm{F,G}}^0$ compared with Figure S7b. Note that in the reverse bias regime, less $|V_\mathrm{b}|$ is required to exert obvious influence over $E_{\mathrm{F,G}}$ than in the forward regime, because once the SG interface layer is weakly inverted, more bias is needed to turn the interface layer to accumulation than to strong inversion. We conclude from energy diagrams in both reverse and forward bias regimes that applying a high $|V_\mathrm{b}|$ will significantly dilute the effect of gating control in a MOGS QC.

References

(S1) Cowley, A. M.; Sze, S. M. *J. Appl. Phys.* **1965**, *36*, 3212–3220.

(S2) Heine, V. *Phys. Rev.* **1965**, *138*, A1689–A1696.

(S3) Sze, S. M.; Ng, K. K. *Physics of Semiconductor Devices*; John Wiley & Sons, Inc., 2006.

(S4) Lui, C. H.; Li, Z.; Mak, K. F.; Cappelluti, E.; Heinz, T. F. *Nat. Phys.* **2011**, *7*, 944–947.

(S5) Regan, W.; Byrnes, S.; Gannett, W.; Ergen, O.; Vazquez-Mena, O.; Wang, F.; Zettl, A. *Nano Lett.* **2012**, *12*, 4300–4304.